Chalcogenide Letters Vol. 22, No. 9, September 2025, p. 765 - 776

Influence of processing parameters on physiochemical properties of cadmium sulfide nanoparticles

S. R. Ahmed [a,*], M. V. V. K. S. Prasad [a], K. Keerthivasan [b]
[a] *Department of Physics, Koneru Lakshmaiah Education Foundation, Guntur, India-522502*
[b] *University of Technology and Applied Science-Utas, Muscat, Oman*

This study focuses on optimizing practical synthesis to produce ultrafine CdS nanoparticles. Three separate chemical synthesis processes, namely microwave, wet-chemical, and sonication methods, are used to generate CdS nanoparticles. Moringa oleifera leaf extract employed green syntheses of CdS nanoparticles are also performed for additional discussions. The generated CdS nanoparticles were subjected to a comparative assessment to identify the most effective processing method for synthesizing CdS nanoparticles. Even though the processing parameters were altered over their synthesis, the hexagonal structure was retained in the CdS nanoparticles. The observed results of CdS nanoparticles from XRD, SEM/EDX, and UV-Vis, according to PSA, the decreased particle size might be attributable to the regulated conditions and temperature used to synthesize CdS nanoparticles utilizing the sonication technique. The observed results revealed the CdS nanostructure property's calibratable nature by its processing parameters and high affectivity in optoelectrical applications.

(Received December 28, 2024; Accepted September 2, 2025)

Keywords: CdS nanoparticles, Physiochemical properties, Opto-electrical applications

1. Introduction

Researchers have tried to develop new organic structures using semiconductor materials to convert light energy with better efficiency. Several attempts have been made to develop new inorganic structures to convert light energy [1-2] effectively. Scientists have been conducting intense research on cadmium sulphide (CdS), a material with numerous possible applications from photovoltaic to fluorescent tubes. Cadmium vacancies caused by extra cadmium atoms cause this important n-type semiconductor to conduct electricity. The CdS nanoparticles exhibit a quantum size effect and are directly related to the absorption wavelength, giving this semiconductor an advantage over other semiconductors with small direct band gaps at lower temperatures [3-4]. Among other things, CdS nanoparticles offer excellent visible light detection properties and are significant in determining optoelectronic qualities. Due to their electronic and optical properties, CdS nanoparticles are ideal quantum-confined semiconductors. It is used as a window material in numerous industrial applications due to its wide band gap, such as photovoltaic cells, batteries, supercapacitors, photocatalytic activities, and anticorrosive materials. It also has properties for such applications in light-emitting diodes, photodetectors, field effect transistors, and sensors [5-8]. Numerous methods have been established to synthesize CdS nanoparticles with divergent morphologies and structures, such as solvothermal, hydrothermal, photoreaction, one-pot synthesis, chemical precipitation, etc. [9-13]. Among them, the green synthesis method is a simple, sparkling, non-hazard and low-cost procedure to acquire CdS nanoparticles compared with other chemical methods [3].

In this research, CdS nanoparticles were synthesized by three different chemical synthesis methods and compared with the Moringa oleifera leaf extract-assisted green synthesis method. The various synthesis methods, such as sonication, wet-chemical, and microwave approaches, are thoroughly investigated for the resulting nanoparticles' phase, structural, optical, and

* Corresponding author: rafeeksra@gmail.com
https://doi.org/10.15251/CL.2025.229.765

morphological aspects. The abovementioned procedures made CdS nanoparticles because of their positive vital points.

Apart from evaluating the above property, we sought to conduct a comparative analysis of the generated CdS nanoparticles for optoelectrical applications in this paper. From the earlier reports, the change in synthesis parameters shows tremendous changes in prepared nanoparticles and their efficiencies in various applications. Furthermore, researchers are interested and highly involved in preparing various nanoparticles using green synthesis methods for increased uses of nanoparticles in energy and environmental applications. This research compares the processing parameters and synthesis processes that can create highly effective nanoparticles for optoelectrical applications.

2. Experimental

2.1. Materials

Cadmium chloride ($CdCl_2$), Sodium Sulphide Flakes (Na_2S) and citric acid were purchased from Merck. To prepare CdS nanoparticles, double distilled water (DD), and *Moringa oleifera* leaves are used.

2.2. Method

The CdS nanoparticles has been produced using the wet-chemical route, and 0.01 M of Cadmium chloride ($CdCl_2$) solution, 0.02 M of citric acid and 0.01 M Sodium Sulphide Flakes (Na_2S) solutions were prepared separately. Citric acid was added dropwise to the cadmium chloride solution, and the solution was stirred for 30 min to get a homogenous solution. After that, sodium sulphite solution was added to the above solution, which resulted in yellow colour, and to improve the reaction with it, the final solution was agitated for 4 hours. The chemical reaction is as follows

$$CdCl_2 + Na_2S \rightarrow CdS + 2\ NaCl$$

The solution was then dried in a hot air oven after the period. The dried encourages were washed with DD water and ethanol to dispose of unreacted compounds. The final sediments were dried at 160 °C in a hot air oven for six hours to make ultrafine CdS nanoparticles. The sample is called CdS-W; the Wet chemical method is spelt W.

2.3. Sonication method

A sonicator with a 40 KHz frequency was used to sonicate the prepared base solution for one hour until an apparent yellow colour suspension resulted. After this suspension of precipitates was obtained, the base solution was dried for 12 hours using an oven at 80°C. For ultrafine CdS nanoparticles, the final sediment was dried in an oven at 160 °C for 6 hours. After repeated washings with fresh water and ethanol, the final sediment was dried for 6 hours. The result was the CdS-S nanoparticles.

2.4. Microwave method

The microwave method was used for the synthesis of CdS nanoparticles. The autoclave was used for preparing the base solution, followed by the microwave oven. It was decided that 900 W Power for 10 mins was the critical parameter for synthesis. Compared to other nanoparticles synthesized using high-temperature synthesis methods, microwave solution exhibits a more regulated pressure and temperature relationship, leading to fewer point defects. Distilled water and ethanol were used to wash the dried precipitates several times before they were dried at 160°C in a hot air oven to obtain CdS nanoparticles. The autoclave was kept undisturbed for cooling before it was transferred to a hot air oven for drying for 12 hours at 80°C. The procured CdS nanoparticles were hereafter termed CdS-M.

2.5. Green synthesis

The healthy and unsullied Moringa oleifera leaves were collected from Ibri, Oman. Moringa oleifera leaves were thoroughly cleansed repeatedly with deionized water (D.D.) to remove dust particles from the leaves' surface, then dried for two weeks at room temperature. To attain leaf extract, 10 grams of dried leaf were placed in 100 mL of D.D. and left for 24 hours. Whatman No. 1 filter paper filters the solution to attain the extract of Moringa oleifera leafs for the green synthesis of CdS nanoparticles. Then, 0.01 M of Cadmium chloride (CdCl2) solution and 0.01 M Sodium Sulphide Flakes (Na2S) solutions were prepared separately. Sodium sulphite solution was dropwise, added to cadmium chloride solution, and stirred for 30 min to get the homogenous solution, resulting in a yellow colour solution.

Later, the solution dried at 80 °C for 12 hours in a hot air oven, and the dried precipitates were washed repeatedly with D.D. and ethanol. Then the final sediments were dried for 6 hours in a hot air oven at 160 °C to get the final nanoparticles. Hereafter, the collected powders will be termed CdS-G.

2.6. Characterisation of CdS nanoparticles

The XRD analysis was performed on XRD instrument (XRD; X'Pert PRO; PANalytical, Almelo, the Netherlands). Rietveld refinement analytical method using FULLPROF software was performed to analyze the lattice parameter and crystal values of the prepared CdS nanoparticles. Fourier transform infrared spectroscopy (Spectrum 100; PerkinElmer, USA) study was performed for functional group identification of the prepared CdS nanoparticles. To study the average particle size distribution, a particle size analyzer (Nanophox; Sympatec, Germany) study was used. To study the optical absorbance of the prepared CdS nanoparticles, UV-Vis spectrometer (Shimadzu U.V.– Visible spectrophotometer, model UV 1800) was used. The band gap of the prepared CdS nanoparticles is calculated using the results of UV-Vis spectroscopy by employing Tauc relations. Surface topology and morphological characteristics of the prepared CdS nanoparticles were studied using Scanning electron microscopy (SEM) in addition to Energy Dispersive X-ray Spectroscopy (EDX) (JEOL JSM-6390LV, Tokyo, Japan) with elemental mapping analysis.

3. Results and discussion

3.1 X-ray diffraction analysis (XRD)

The X-ray diffraction (XRD) patterns (Figure 1) for all the CdS nanoparticles were varied. It reveals a hexagonal crystal structure for all synthesized nanoparticles with well-defined lattice planes, indicating crystalline. They are in good agreement with the hkl planes of (100), (000), (101) and (110) at 2θ=24.8°, 26.5°, 28.1° and 47.8° which are signature markers of hexagonal CdS pattern (JCPDS card No: 41-1049) [14]. Furthermore, the figure contends that the intensity of the peak increases in the order of wet-chemical, microwave, as well as sonication methods and decreases for green synthesis methods, implying that CdS nanoparticles synthesized via the sonication process have higher crystallinity than CdS nanoparticles synthesized via the other three methods, implying that CdS nanoparticles could be tuned by changing the processing conditions [15]. The average crystalline size of CdS nanoparticles was calculated using the Scherer equation, $D= (K\lambda/\beta D\cos\theta)$. Here k represents constant 0.89, λ represents the wavelength of the x-ray, θ is the angle of diffraction, and β refers to full-width half maxima [16].

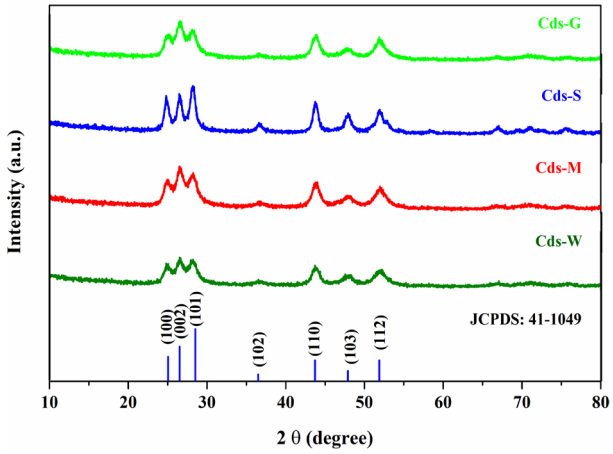

Fig. 1. Shows the XRD spectrum of CdS-W, CdS-M, CdS-S and CdS-G nanoparticles.

Here, the Debye-Scherer estimation was used to calculate the average particle size discovered due to changing one processing parameter to another. When compared to nanoparticles synthesized using wet-chemical (16.43 nm), microwave (12.95), and green (15.36 nm) procedures, CdS nanoparticles synthesized using sonication (CdS-S) as the processing parameter have an extraordinarily tiny size of roughly 12.15 nm.

Table 1. Gives structural details and calculated average crystal size of the CdS nanoparticles from XRD analysis.

(hkl)	**FWHM (rad)**				**2 θ (°)**	**Crystal size (nm)**			
	CdS-W	CdS-M	CdS-S	CdS-G		CdS-W	CdS-M	CdS-S	CdS-G
(100)	0.6022	0.6691	0.6602	0.6691	24.9644	13.51	12.15	12.31	12.15
(002)	0.6022	0.6022	0.6353	0.4684	26.6459	13.55	13.55	12.44	17.42
(101)	0.5346	0.5353	0.6453	0.6022	28.0408	15.31	15.30	12.68	13.59
(102)	0.6022	0.8029	0.6691	0.4684	43.8047	14.21	10.66	12.78	18.28
Average Crystal size						16.43	12.95	12.15	15.36

CdS nanoparticles (CdS-W, CdS-M, CdS-S, and CdS-G) synthesized using various methods are generally polycrystalline. As a result, in our reports, the nanoparticles were prepared at 160 °C to ensure an effective induce to crystallization of CdS nanoparticles. The CdS nanoparticles' X-ray diffraction is shown in Figure 1. The indexed miller indices of each Bragg peak confirm the crystalline nature of the produced CdS nanoparticles.

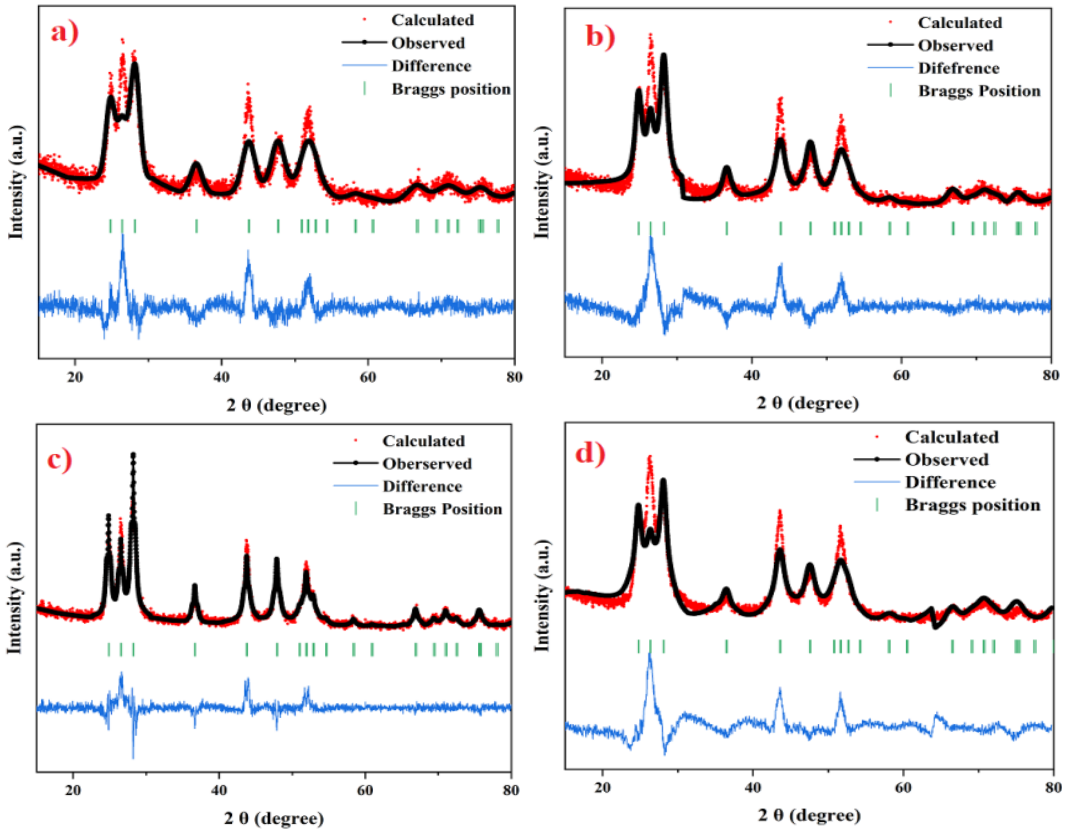

Fig. 2. Refinement results of CdS nanoparticles (a: CdS-W, b: CdS-M, c: CdS-S and d: CdS-G).

The CdS nanostructure of Rietveld refinement spectra is shown in figure 2. The CdS nanostructure shows the space group of P63mc (186). With the help of refinement, the crystal structures are calculated [17-19]. The CdS nanoparticles of calculated refine parameters (CdS-W, CdS-M, CdS-S and CdS-G) are shown in table 2. A slight in the crystal parameters were observed due to a change in processing parameter during the synthesis process. The change in cell parameters for CdS-W, CdS-M, CdS-S and CdS-G nanoparticles were shown in Tables 3–6, respectively.

Table 2. Gives the refine results of CdS nanoparticles.

Space group: P63mc (186), Structure: Hexagonal							
Sample	a =b (Å)	c (Å)	Volume (Å)	Rp	Rwp	Rexp	χ2
CdS-W	4.141	6.75	100.29	11.3	14.7	10.4	1.98
CdS-M	4.132	6.73	99.57	14.4	17.1	9.57	1.4
CdS-S	4.135	6.71	99.49	10.6	13.5	9.94	1.8
CdS-G	4.153	6.76	101.12	14.5	18.1	9.89	1.33

Table 3. The Cell parameter of CdS-W nanoparticles.

Atom	x	y	z	Biso	Occ
Cd	0.333	0.666	0	0	0.16667
S	0.333	0.666	0.375	0	0.16667

Table 4. The Cell parameter of CdS-M nanoparticles.

Atom	x	y	z	Biso	Occ
Cd	0.333	0.666	0	0	0.16667
S	0.333	0.665	0.374	0	0.16667

Table 5. The Cell parameter of CdS-S nanoparticles.

Atom	x	y	z	Biso	Occ
Cd	0.333	0.666	0	0	0.16667
S	0.333	0.664	0.376	0	0.16667

Table 6. The Cell parameter of CdS-G nanoparticles.

Atom	x	y	z	Biso	Occ
Cd	0.333	0.666	0	0	0.16667
S	0.333	0.663	0.375	0	0.16667

3.2. Thermo gravimetric analysis (TG)

The profile curves produced by thermogravimetric analysis (TGA) on the prepared CdS-W, CdS-M, CdS-S, and CdS-G nanoparticles are shown in Figure 3. At 100 °C (I), 480 °C (II), and 720 °C (III), the TGA curve exhibits three significant weight losses. The minor weight loss (I) in the low-temperature zone indicates the presence of a water molecule in the lattice. The TGA bend for CdS-M and CdS-S tests show an unexpected weight reduction of around 29.7 and 28.7 % in the temperature scope of 450 to 500 K, separately, though CdS W and CdS G show minor shedding pounds just in the TGA bend.

From the beginning of the analysis, the retained weight percent of the prepared CdS-W, CdS-M, CdS-S, and CdS-G nanoparticles is 52.5, 50.2, 56.8, and 49.05 %, respectively. Compared to wet-chemical, microwave, and green synthesis methods, these results show that the sonication process produces highly thermally stable CdS nanoparticles. Weight loss is caused by the evaporation of water and organic components in the synthesized CdS nanoparticles' degradation. CdS nanoparticles have previously been observed to cause weight loss [20-21].

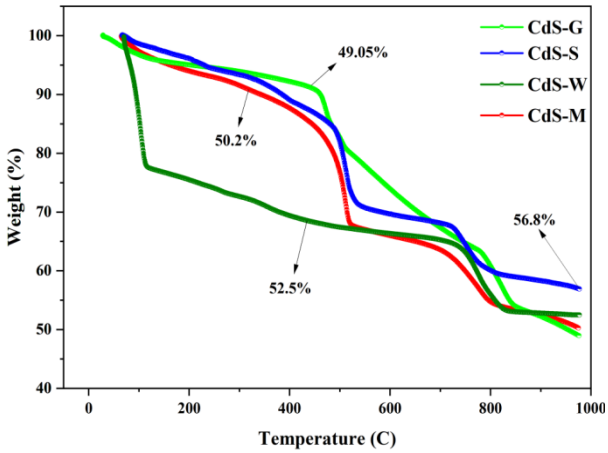

Fig. 3. Thermal gravimetric analysis of the prepared CdS-W, CdS-M, CdS-S and CdS-G nanoparticles.

3.3. Fourier transforms infrared spectra (FTIR)

Figure 4 illustrates the FTIR spectra of the prepared CdS-W, CdS-M, CdS-S, and CdS-G nanoparticles. As you can see in the graph, this band is associated with the CdS band at 630-640 cm^{-1} [22]. Molecular vibrations of the hydroxyl molecule can be seen at 1120, 1670, and 3368 cm^{-1}. CH_2 stretching and bending vibrations are realized at 1414 and 2928 cm^{-1}. A sharp peak was observed for all samples at 1640–1650 cm^{-1} owed to stretching vibrations of C=O [23-24].

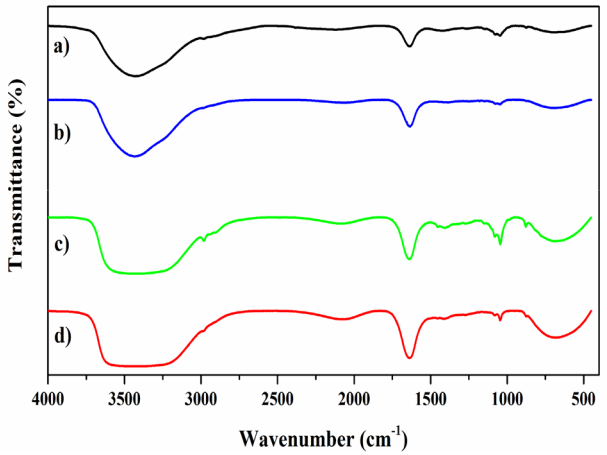

Fig. 4. FTIR spectra of CdS-W, CdS-M, CdS-S and CdS-G nanoparticles.

3.4. Particle size analysis (PSA)

Figure 5 represents the particle size distribution of nanoparticles like CdS-W, CdS-M, CdS-S and CdS-G. The prepared nanoparticles' average particle size (d50) is between 15-25 nm. Moreover, the mean particle size distribution (d50) of CdS-W, CdS-M, CdS-S and CdS-G nanoparticles is 23.04±2, 22.2±2, 21.5±2 and 19.1±2 nm, respectively. The preparation of all the CdS nanoparticles under different processing parameters directly influences the formation of the particles at the nanoscale level [25-26]. The CdS-S nanostructure shows smaller particle sizes than CdS-W, CdS-M, and CdS-G, as evidenced by the crystallographic peaks and the calculated parameters from XRD results.

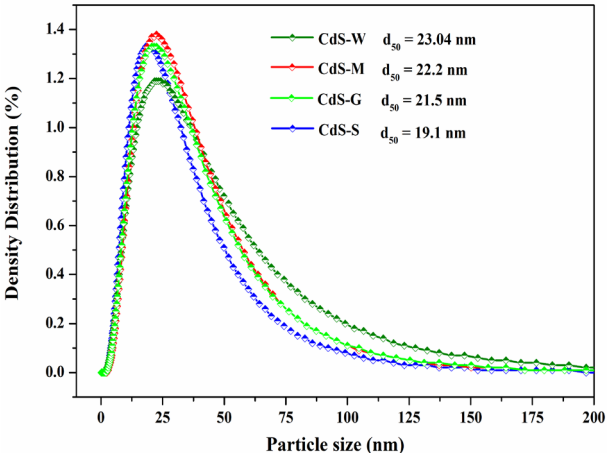

Fig. 5. The average particle distribution of CdS-W, CdS-M, CdS-S and CdS-G nanoparticles.

3.5. Morphological analysis (SEM)

Figure 6 shows the surface morphological images and their corresponding EDX spectra of the obtained CdS nanoparticles. Agglomerated particles and an irregular form can be noticed in the CdS nanoparticles generated by the wet-chemical technique. On the other hand, the CdS nanoparticles made by the microwave approach have a greater dispersity and a more mixed rod-like structure, which can be attributed to the microwave method's ability to modify the shape and prevent nanoparticle aggregation readily.

It also exhibits a narrow particle size distribution, with an average diameter of roughly 20 nm, similar to the XRD pattern and average particle size distribution results. Both CdS-S (Wet-chemical) and CdS-M (microwave) nanoparticles have indistinguishable morphology in Figures 6a and b, but CdS-S (sonication) and CdS-G (green synthesis) nanoparticles have distinct aggregated spherical structured nanoparticles in Figures 6c and 6d. The spherical form exhibited solely in CdS-S nanoparticles could be due to the influence catalysed conversion of cadmium chloride to cadmium nanoparticles caused by regulated sonication power and temperature during the synthesis procedure.

3.6 Optical analysis (UV-Vis)

The UV-Vis absorption spectra of CdS-W, CdS-M, CdS-S, and CdS-G nanoparticles are depicted in Figure 6a, and 6b shows the UV-Vis transmittance spectra of it. In the spectra, absorption peaks of microscopic intensity began at about 220 nm, shown in fig. 6a. In the experiment, the broad absorption peaks intensity decreases as a change in influencing factors and the peaks are moved towards a lower wavelength [27-28]. It is important to note that nanoparticles' particle size significantly impacts their optical qualities. When absorption begins, the UV-Vis spectra show a blue shift with a decrease in crystallite size. [29].

The blue shift absorption spectra are the direct result of the relationship between particle size and quantum confinement. When there is an increase in bandgap and a decrease in particle size, the quantum confinement effect occurs, which causes absorption spectra to shift toward shorter wavelengths.

Bandgap energy is derived from absorption spectra using the Tauc relation, shown in Figure 6 (c and d). Using the following equation, the absorption coefficient of semiconductor nanoparticles is related to the incident photon energy [30]

$$\alpha\,(\upsilon) = K\,(h\upsilon\, -\, E_g\,)^n$$

$\alpha\,(\upsilon)$ Represents Absorption coefficient, K is constant, Eg refers to the bandgap energy, $h\upsilon$ represents the incident photon energy and where n equals ½ and 2 for direct and indirect band gap semiconductors.

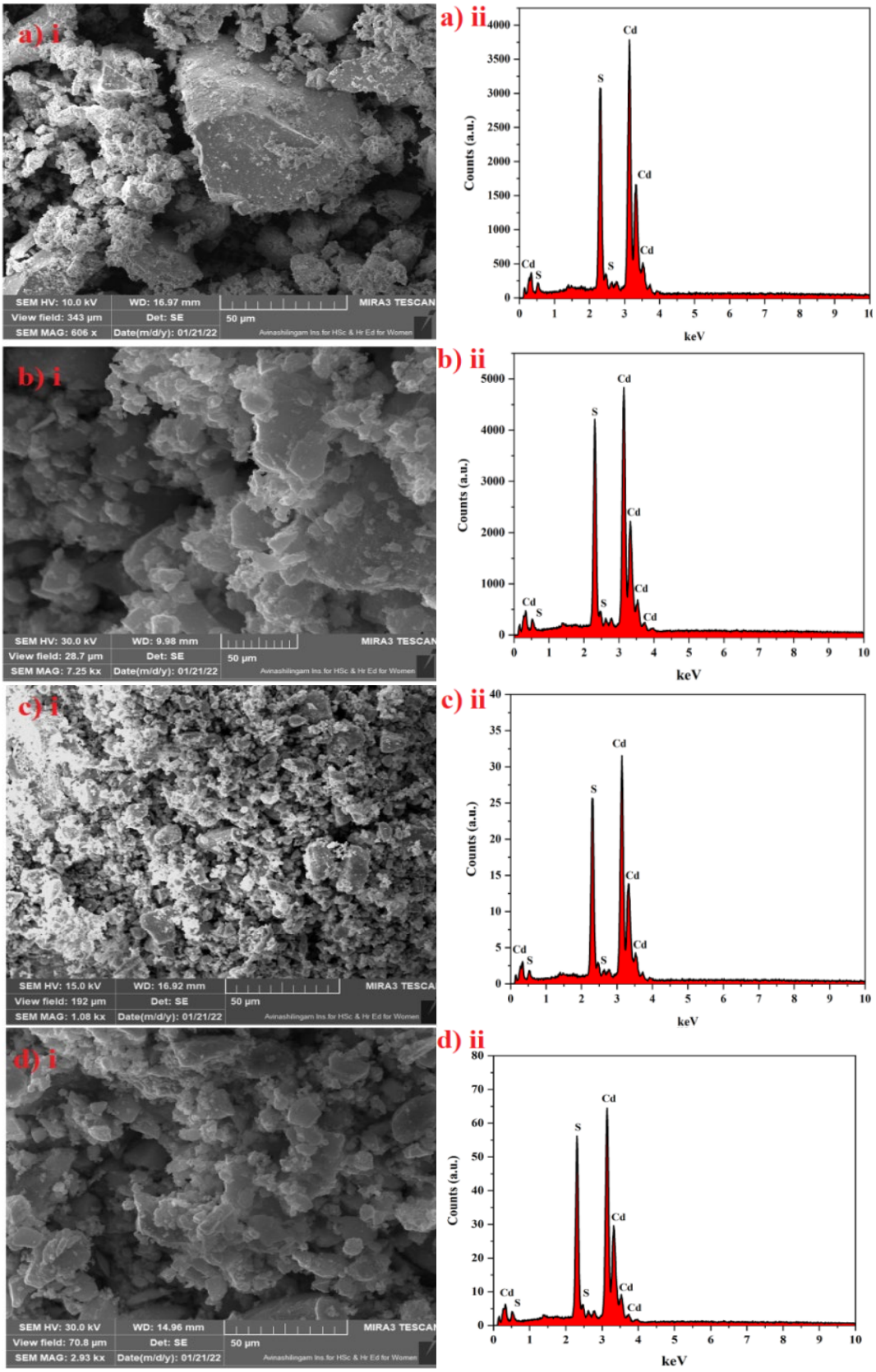

Fig. 6. The SEM images and EDX spectra of CdS-W (a), CdS-M (b), CdS-S (c) and CdS-G (d) nanoparticles.

Table 7 lists the bandgap energies calculated for CdS-W, CdS-M, CdS-S, and CdS-G nanoparticles. A precise match exists between the calculated energy bandgap values and the earlier reports [31-32]. CdS-W, CdS-M, CdS-S, and CdS-G nanoparticles show the same energy bandgap (2.73-2.78 eV) calculated from Tauc relationships for all the samples based on UV-Vis absorbance spectra. Nevertheless, the CdS-G nanostructure absorbs U.V. light at a greater intensity than the other three nanoparticles (CdS-W, CdS-M, and CdS-S).

Table 7. Size and bandgap assessment on CdS-W, CdS-M, CdS-S, and CdS-G nanoparticles.

Sample	Crystal size (nm)	Particle size (nm)	Energy Bandgap (eV) by Tauc plot	
			Direct	Indirect
CdS-W	16.43	23.04	2.77	2.51
CdS-M	12.95	22.2	2.73	2.51
CdS-S	12.15	21.5	2.78	2.49
CdS-G	15.36	19.1	2.78	2.50

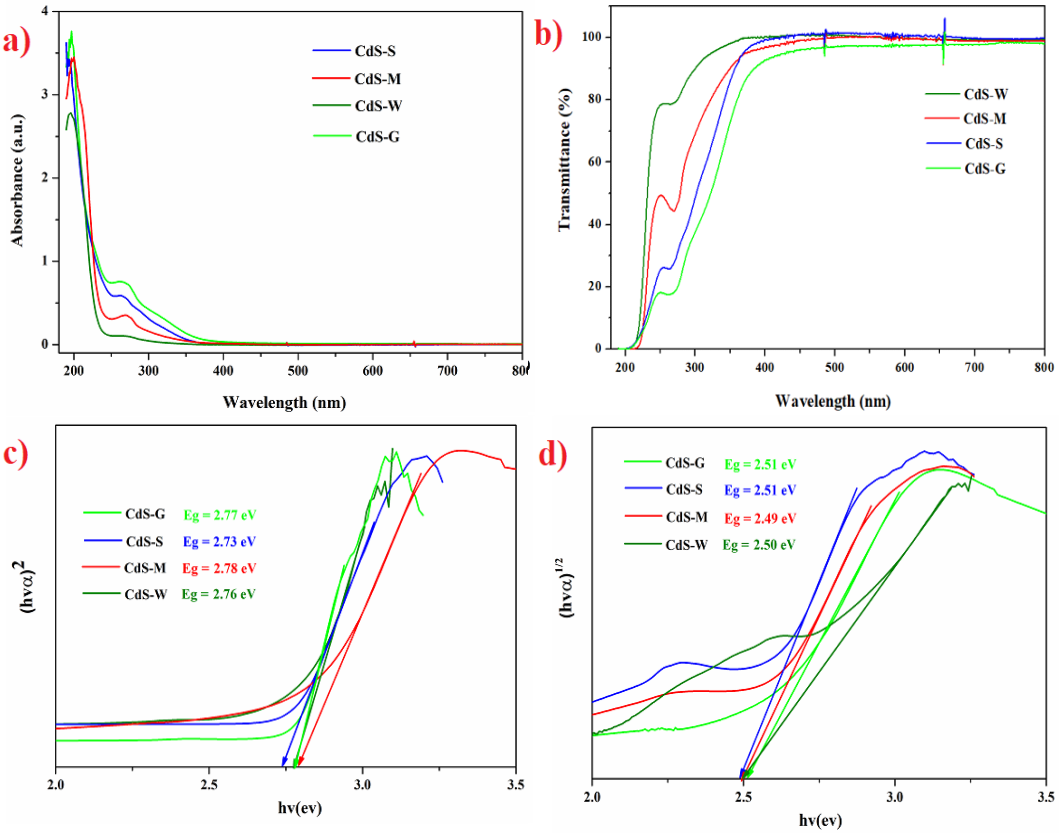

Fig. 6. (a) UV-Vis absorbance spectra, (b) UV-Vis Transmittance, (c) Tauc plot-Direct bandgap and (d) Tauc plot-Indirect bandgap of the prepared CdS-W, CdS-M, CdS-S and CdS-G nanoparticles.

4. Conclusion

The CdS-W, CdS-M, CdS-S, and CdS-G nanoparticles were produced using cadmium chloride and sodium sulphate as precursor materials and citric acid as stabilizing agent by varying the four different synthesis methods like, wet chemical, sonication, microwave and green synthesis. When compared to the other three methods, the sonication process (CdS-S) nanoparticles exhibit excellent crystallinity and nanoparticles with smaller crystallite and particle sizes.

The particle sizes of the prepared CdS nanoparticles are slightly reduced due to the different influencing processes. In addition to FTIR and FESEM with EDAX analysis, other physicochemical analyses have shown that CdS nanoparticles are well-formed. The FESEM images demonstrated that the synthesis parameters significantly influenced CdS morphology. The nanoparticles are free of impurities based on EDAX and elemental mapping results. CdS-G and CdS-S exhibit the highest absorbance ratio compared to the other two samples. As demonstrated in the brief experimental evaluations above, the synthesized CdS nanoparticles by the sonication process have excellent properties compared to all three samples. Furthermore, this comparative assessment enables a better understanding of how different processing methods impact the structural, morphological, and optoelectronic properties of CdS nanoparticles, which helps tailor nanoparticles for various applications.

References

[1] S. Arya, A. Sharma, B. Singh, M. Riyas, P. Bandhoria, M. Aatif, V. Gupta, Opt. Mater. 79 (2018) 115–119; https://doi.org/10.1016/j.optmat.2018.03.035
[2] D.G. Moon, S. Rehan, D.H. Yeon, S.M. Lee, S.J. Park, S. Ahn, Y.S. Cho, Sol. Energy Mater Sol. Cell. 200 (2019) 109963; https://doi.org/10.1016/j.solmat.2019.109963
[3] V. Kavitha, P. Mahalingam, M. Jeyanthinath, N. Sethupathi, Mater. Today-Proc. 23 (2020) 12-15; https://doi.org/10.1016/j.matpr.2019.05.351
[4] V. Kavitha, P. Mahalingam, M. Jeyanthinath, N. Sethupathi, Mater Today-Proc. 35 (2021) 48-52; https://doi.org/10.1016/j.matpr.2019.05.437
[5] Ning Du, Y. Cui, L. Zhang, M. Yang, Phys. Chem. Chem. Phys.; https://doi.org/10.1021/acs.jpcc.1c00970
[6] K. Veerathangam, M.S. Pandian, P. Ramasamy, Mater. Lett. 220 (2018) 74-77; https://doi.org/10.1016/j.matlet.2018.03.007
[7] D.S. Ahmed, M.K. A. Mohammed, S.M. Majeed, ACS Appl. Energy Mater.; https://doi.org/10.1021/acsaem.0c01896
[8] N.K. Tailor, M. Abdi-Jalebi, V. Gupta, Hanlin Hu, M.I. Dar, Gang Li, S. Satapathi, J. Mater. Chem. A, 2020, 8, 21356; https://doi.org/10.1039/D0TA00143K
[9] S. Karthikeyan, K. Dhanakodi, S. Surendhiran, P. Thirunavukkarasu, L. Arunraja, and P. Manojkumar, AIP Conf. Proc. 2022; 2385: 020004; https://doi.org/10.1063/5.0070786
[10] S. Ambika, S. Gopinath, K. Saravanan, K. Sivakumar, C. Ragupathi, T.A. Sukantha, Energy Rep. 5 (2019) 305-309; https://doi.org/10.1016/j.egyr.2019.02.005
[11] Majeed, Sadeer M., Mustafa KA Mohammed, and Duha S. Ahmed. Applied Physics *A* 129.7 (2023): 470; https://doi.org/10.1007/s00339-023-06749-0
[12] D. Vasudevan, D. Senthilkumar, S. Surendhiran, Int. J. Thermophys. 41:74 (2020) 1-19; https://doi.org/10.1007/s10765-020-02651-6
[13] Peng, Z., Luo, W., Long, C., Wang, Y., & Fu, Y. (2023), Applied Physics A, 129(1), 54; https://doi.org/10.1007/s00339-022-06330-1
[14] S. Karthikeyan, P. Thirunavukkarasu, S. Surendhiran, A. Balamurugan, Y. A. Syed Khadar, AIP Conf. Proc. 2022; 2385: 020003; https://doi.org/10.1063/5.0070921
[15] R.A. Devi, M. Latha, S. Velumani, G. Oza, P. Reyes-Figueroa, M. Rohini, I. G. Becerril-Juarez, J. Lee, Junsin Y, J. Nanosci. Nanotechnol, Vol. 15, 8434–8439, 2015; https://doi.org/10.1166/jnn.2015.11472
[16] S. Karthikeyan, K. Dhanakodi, K. Shanmugasundaram, S. Surendhiran, Mater. Today: Proc. 2021; 47: 901-906; https://doi.org/10.1016/j.jics.2023.101104
[17] H.S. Mahdi, A. Parveen, A. Azam, AIP Conference Proceedings 1953, 030031 (2018); https://doi.org/10.1063/1.5032366
[18] Evazinejad-Galangashi, R., Mohagheghian, A., & Shirzad-Siboni, M. (2024), Journal of Environmental Management, 368, 122043; https://doi.org/10.1016/j.jenvman.2024.122043
[19] S. Karthikeyan, P. Thirunavukkarasu, S. Surendhiran, Y.A. Syed Khadar, A. Balamurugan, B. Gobinath, Mater. Today:Proc. 2021; 47: 970-977; https://doi.org/10.1016/j.matpr.2021.05.217

[20] Rahman, M. F., Hossain, J., Kuddus, A., Tabassum, S., Rubel, M. H., Shirai, H., & Ismail, A. B. M. (2020). Applied Physics A, 126, 1-11; https://doi.org/10.1007/s00339-020-3331-0
[21] M. Thambidurai, N. Muthukumarasamy, S. Agilan, N. Sabari Arul, N. Murugan, R. Bala sundaraprabhu J. Mater. Sci. (2011) 46:3200–3206; https://doi.org/10.1007/s10853-010-5204-y
[22] A. Badawi, N. Al-Hosiny, S. Abdallah, Superlattice Microst, 81 (2015) 88–96; https://doi.org/10.1016/j.spmi.2015.01.024
[23] K. C. Suresh, S. Surendhiran, P. Manoj Kumar, E. Ranjth Kumar, Y. A. Syed Khadar, A. Balamurugan, SN Appl. Sci. 2 (2020) 1-13; https://doi.org/10.1007/s42452-020-03534-z
[24] K. Kandasamy, S. Surendhiran, Y.A. Syed Khadar, P. Rajasingh, Mater. Today-Proc. 47 (2020) 757-762; https://doi.org/10.1016/j.matpr.2020.07.080
[25] A. Balamurugan, M. Sudha, S. Surendhiran, R. Anandarasu, S. Ravikumar, Y.A. Syed Khadar, Mater. Today-Proc. 26:4 (2020) 3588-3594; https://doi.org/10.1016/j.matpr.2021.04.335
[26] Tinedert, I. E., Pezzimenti, F., Megherbi, M. L., & Saadoune, A. (2020), Optik, 208, 164112; https://doi.org/10.1016/j.ijleo.2019.164112
[27] Badawi, A., & Alharthi, S. S. (2022). Applied Physics A, 128(4), 328; https://doi.org/10.1007/s00339-022-05495-z
[28] Li, X., Liu, H., Ke, C., Tang, W., Liu, M., Huang, F., Kang, J. (2021). Laser & Photonics Reviews, 15(12), 2100322; https://doi.org/10.1002/lpor.202100322.
[29] Li, P., Zhou, Z., Zhao, Y. S., & Yan, Y. (2021). Chemical Communications, 57(100), 13678-13691; https://doi.org/10.1039/D1CC05541K
[30] Feng, J., Li, X., Zhu, G., & Wang, Q. J. (2020). ACS applied materials & interfaces, 12(38), 43098-43105; https://doi.org/10.1021/acsami.0c12907
[31] S. Karthikeyan, P. Thirunavukkarasu, S. Surendhiran, A. Balamurugan, Y.A. Syed Khadar, K. Shanmugasundaram, Mater. Today: Proc. 2021; 47: 964-969; https://doi.org/10.1016/j.matpr.2021.05.194
[32] C. N. Omprakash Anand, P. Thirunavukkarasu, S. Surendhiran, A. Balamurugan, K. C. Suresh, Y. A. Syed Khadar, AIP Conf. Proc. 2022; 2385: 020007; https://doi.org/10.1063/5.0070919